ORIGINAL CONTRIBUTION

EXPERIMENTAL ONCOLOGY

https://doi.org/10.15407/exp-oncology.2025.01.024

V. BRICHENKO [1], L. SHLAPATSKA [2], M. ZAVELEVICH [2], L. ZVARYCH [1], V. PANCHENKO [1], O. LYASKIVSKA [1], O. SKACHKOVA [3], N. GOLYARNIK [1], I. ABRAMENKO [1, *], L. BUCHYNSKA [2], A. CHUMAK [1]

[1] National Research Center for Radiation Medicine, Hematology and Oncology, the National Academy of Medical Sciences of Ukraine, Kyiv, Ukraine

[2] R.E. Kavetsky Institute of Experimental Pathology, Oncology and Radiobiology, the National Academy of Sciences of Ukraine, Kyiv, Ukraine

[3] Nonprofit organization "National Cancer Institute", Kyiv, Ukraine

* Correspondence: Email: abramenko_iryna@ukr.net

EFFECTS OF SARS-COV-2 SPIKE PROTEIN ON THE GROWTH AND PHENOTYPE OF MDA-MB-231 AND MCF-7 BREAST CANCER CELLS AND THEIR SENSITIVITY TO RADIATION-INDUCED APOPTOSIS

Background. The coronavirus infection caused by SARS-Cov-2 virus, in addition to the development of severe acute respiratory syndrome, is responsible for the development of a multiple organ dysfunction syndrome. An important aspect is its relationship with cancer. The data from clinical and experimental studies are contradictory. Thus, further studies are needed to elaborate on the potential effects of SARS-Cov-2 on cancer cells. **Aim**. To study the effect of SARS-Cov-2 spike protein (SP) on the survival, phenotype, and sensitivity to radiation-induced apoptosis of breast cancer (BC) cell lines of different molecular subtype (MDA-MB-231 and MCF-7). **Materials and Methods**. The effects of SARS-Cov-2 SP on MDA-MB-231 and MCF-7 cells were assessed using the cell proliferation assay and flow cytometry (Ki-67, CD44, CD133, CD105, CD90, CD10, CD5, CD19, and p53). The sensitivity to radiation-induced apoptosis was evaluated by 7-amino-actinomycin D and propidium iodide staining. **Results**. We did not find any significant short-term effect of SP on the proliferative activity of both studied cell lines. The phenotype of MDA-MB-231 cells cultured with SP changed toward a decrease in $CD105^+CD90^+$ and $CD105^+CD90^-$ subpopulations ($p < 0.0001$). The p53 expression increased both in SP-treated MDA-MB-231 and MCF-7 cells. The sensitivity of SP-treated MDA-MB-231 and MCF-7 cells to radiation-induced apoptosis, although insignificantly, increased. Apoptosis in irradiated MDA-MB-231 cells was accompanied by a two-fold increase in the fluorescence intensity of p53 in SP-treated MDA-MB-231 cells. In both irradiated cultures, a significant increase in the percent of cells in S-phase after SP treatment was observed compared to SP-untreated cells. **Conclusion**. Since most vaccines are based

Citation: Brichenko V, Shlapatska L, Zavelevich M, Zvarych L, Panchenko V, Lyaskivska O, Skachkova O, Golyarnik N, Abramenko I, Buchynska L, Chumak A. Effects of SARS-COV-2 spike protein on the growth and phenotype of MDA-MB-231 and MCF-7 breast cancer cells and their sensitivity to radiation-induced apoptosis. *Exp Oncol*. 2025; 47(1): 24-33. https://doi.org/10.15407/exp-oncology.2025.01.024

on SP expression, the obtained data might have a certain significance in the study of the effect of anti-SARS-Cov-2 vaccination on tumor growth and the sensitivity of cancer cells to cytoreduction therapies.

Keywords: MDA-MB-231 and MCF-7 cell lines, SARS-Cov-2, spike protein, immunophenotype, radiation-induced apoptosis, cell cycle.

The coronavirus infection (COVID-19, COronaVIrus Disease 2019), caused by new strains of the SARS-Cov-2 virus (severe acute respiratory syndrome-related coronavirus 2), has formulated new challenges for public healthcare. In addition to the development of severe acute respiratory syndrome, evidence has emerged that SARS-Cov-2 is responsible for the development of a multiple organ dysfunction syndrome, the main manifestations of which are nervous disorders (cognitive disorders, fatigue, anxiety, depression), disorders of the cardiovascular system, autoimmune diseases, etc. [1—7]. An important aspect is the relationship between coronavirus infection and cancer. First, oncological and oncohematological patients have an increased risk of severe COVID-19 illness and adverse outcomes [8—11]. On the other hand, it has been hypothesized that SARS-Cov-2 infection increases the risk of tumor development and/or promotes cancer progression [12]. Using the Mendelian randomization method, the association between genetic predisposition to COVID-19 and the risk of 4 types of cancers including HER2-positive breast cancer (BC) in the European population was predicted [13]. There are data on the progression of chronic lymphocytic leukemia in a significant part of patients after a coronavirus infection [14—16]. The MDA-MB-231 BC cell line treated by M protein of SARS-Cov-2 showed increased mobility, proliferation, stemness, and in vivo metastasis as well as the upregulation of NF-κB and STAT3 pathways [17]. However, there are contrary data. In particular, the growth of the prostate cancer LNCaP cells and SiHa cervical cancer cells was suppressed by SARS-Cov-2 spike protein (SP) [18, 19]. Thus, further studies are needed to elaborate on the potential effects of SARS-Cov-2 and its proteins on other cancer cell lines. The aim of our work was to study the effect of SARS-Cov-2 SP on the survival, phenotype, and sensitivity to radiation-induced apoptosis of BC cell lines of different molecular subtypes (MDA-MB-231 and MCF-7).

Materials and Methods

Cell lines. MDA-MB-231 and MCF-7 human BC cell lines were obtained from the Bank of Cell Lines from Human and Animal Tissues of the R.E. Kavetsky Institute of Experimental Pathology, Oncology and Radiobiology of the NASU (Kyiv, Ukraine). The cells were maintained in a DMEM medium (BioWest, France) supplemented with 10% heat-inactivated fetal bovine serum (FBS), 2 mM L-glutamine, 100 U/mL penicillin, and 100 μg/mL streptomycin (Invitrogen, USA). The cells were cultivated in a humidified 5% CO_2 incubator at 37 °C.

Treatment with SARS-Cov-2 SP. The recombinant SP of SARS-Cov-2 (Sino Biological, N 40592-V08H121), which corresponds to the B.1.1.529 variant (Omicron), was used in the study. This SP was used given the widespread distribution of the omicron variant and its subtypes in the world [20]. 100 μg of lyophilized SP was dissolved in DMEM with 10% FBS, stocked in Eppendorf tubes, and stored at –20 °C. The cells were treated with SP at a concentration of 40 pmol/mL.

Cell viability and proliferation assays. A colorimetric assay with crystal violet was performed for the analysis of cell growth and viability [21]. MDA-MB-231 and MCF-7 cells were seeded into the wells of a 96-well plate (1×10^4 cells/100 μL/well) in DMEM + 10% FBS and incubated for 24 h before being treated with SP at a concentration of 60 pmol/mL. After 24, 48, and 72 h of incubation with SP, the cell density was determined using a Crystal Violet Assay Kit (Abcam, USA). The absorbance was measured at a wavelength of 540 nm in a LabSystem Multiscan Plus multiwell reader (Thermo Fisher Scientific, Finland). Additionally, the viability of cells was evaluated by 7-amino-actinomycin D (7-AAD) staining. Cell suspension was incubated with a 7-AAD viability staining solution (Thermo Fisher Scientific, USA) for 5 min followed by the analysis on a BD FACSLyric laser flow cytometer (Becton Dickinson, USA) to discriminate between dead and viable cells.

Immunophenotyping. Surface antigen expression was assessed after 48 h of incubation with/without SP by a direct immunofluorescent method using monoclonal antibodies, conjugated with fluorochromes: FITC (fluorescein isothiocyanate), PE (phycoerythrin), or PerCP-Cyanine 5.5 (PerCP-Cy5.5).

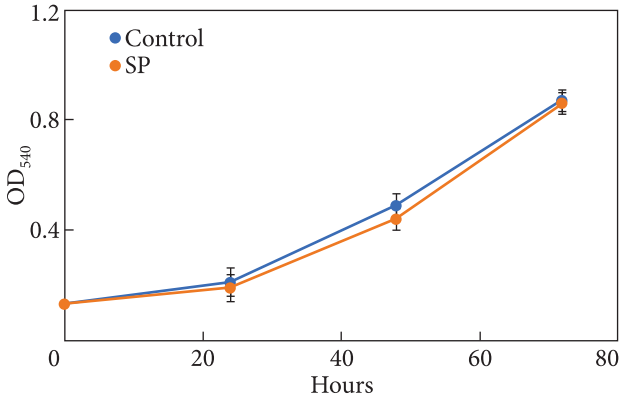

Fig. 1. The effect of SP on the growth of MDA-MB-231 cells. The cells were seeded into the wells of a 96-well plate, and SP was added 24 h later. The cell density at the indicated time points was assessed by crystal violet staining of the cell monolayer. The OD_{540} values were proportional to the cell densities in the wells. All measurements at each time point were made in triplicates

Expression of intracellular antigens was determined using BD Biosciences protocol of staining intracellular antigens for flow cytometry. The following monoclonal antibodies were used: anti-CD133-PE (clone W6B3C1), anti-CD105-PerCP-Cy5.5 (clone 255), anti-CD5-FITC/CD10-PE/CD19-PerCP-Cy5.5 (lot 0338419), anti-p53-FITC (lot 5017633), and anti-CD90-FITC (clone 5E10) — all Becton Dickinson, USA; anti-CD44-FITC (clone IM7, eBioscience, USA) and anti-Ki-67-FITC (clone 20Raj1, eBioscience, USA). The study was performed using a BD FACSLyric laser flow cytometer (Becton Dickinson, USA) using BD FACSuite software (BD, USA) and Beckman Coulter DxFLEX (Beckman Coulter, USA) using CytExpert (DxFLEX Software) for up to 100,000 events in the Dot plot and Dot histogram modes. The level of antigen expression was determined by the median fluorescence intensity (MFI).

Irradiation of cells was performed using a RADGIL2 X-Ray irradiator (Gilardoni, Italy) after 48 h of incubation with and without SP. MDA-MB-231 and MCF-7 cells were irradiated at the doses of 10 Gy for the assessment of p53 expression or 15 Gy for the analysis of apoptosis and cycle traverse at a dose rate of 0.89 Gy/min at room temperature. Cell death was evaluated by 7-AAD staining.

Apoptosis and cell cycle analysis. Apoptosis and cell cycle distribution were analyzed by the propidium iodide (PI) flow cytometric assay [22]. The cells were detached from the plastic surface with EDTA-trypsin solution, washed with PBS, fixed in cold 70% ethanol, then washed twice with PBS, and resuspended in a hypotonic lysis buffer (0.1% sodium citrate, 0.1% Triton X-100, 5 μg/mL propidium iodide). 250 μg/mL of RNase A was added to each cell sample. Flow cytometry was performed on a FACScan flow cytometer (Becton Dickinson, USA), and data were analyzed using ModFit LT 2.0 (Verity Software House, USA) and CELLQuest software (BD Biosciences, USA). At least 20,000 cells were used in each analysis, and the results were displayed as dot plots and histograms. The dead cells and cell debris were eliminated based on forward and side light scatter.

Statistical analysis. Each experiment was replicated independently three times. Data are presented as the percentage of positive cells (M ± m). Statistical analysis was performed with SPSS software (version 17.0; SPSS, Inc., USA). All statistical tests were two-sided and considered to be statistically significant at $p < 0.05$.

Immunophenotype of MDA-MB-231 and MCF-7 cells without and with SP treatment

Antigens	MDA-MB-231 cells, %	MDA-MB-231 cells + SP, %	MCF-7 cells, %	MCF-7 cells + SP, %
CD133	67.27 ± 1.28	65.53 ± 1.83	94.56 ± 1.12	91.16 ± 3.92
CD44	95.25 ± 1.18	95.13 ± 1.27	ND	ND
Ki-67	32.87 ± 2.13	34.35 ± 3.37	13.3 ± 2.1	12.9 ± 1.19
p53	19.21 ± 2.16	43.18 ± 1.97**	0.57 ± 0.08	5.83 ± 1.01*
CD10	0.93 ± 0.35	1.4 ± 0.73	1.41 ± 0.13	5.87 ± 0.69*
$CD90^+CD105^+$	30.51 ± 2.16	23.41 ± 4.21*	0	0
$CD90^-CD105^+$	41.57 ± 2.19	9.47 ± 1.18**	0.17 ± 0.09	0.25 ± 0.11
$CD90^+CD105^-$	0	0	0.49 ± 0.11	0.37 ± 0.08

Notes: ND — antigen expression was not determined; * $p < 0.001$ compared between cell lines without and with SP treatment; ** $p < 0.0001$ compared between cell lines without and with SP treatment.

Results

The SP effects on the growth of BC cells and their immunophenotype were studied.

The incubation of MDA-MB-231 cells in the presence of SP for 72 h did not affect cell growth and the cell density at the end of incubation (Fig. 1). The same was true for MCF-7 cells.

The data on the phenotype of MDA-MB-231 and MCF-7 cells are summarized in the Table.

The MDA-MB-231 cells were characterized by the expression of CD133, CD44, CD105, and CD90 antigens (Table). All $CD90^+$ cells co-expressed the CD105 antigen. Two separate subpopulations were found: $CD90^+CD105^+$ and $CD90^-CD105^+$ cells. The percent of the CD10-positive cells was low, while CD5 or CD19 antigens were not detected.

After SP treatment, the expressions of CD133, CD44, and Ki-67 on the MDA-MB-231 cells did not change, while the expressions of CD105 and CD90 antigens were significantly reduced, resulting in a decrease in the content of both $CD90^+CD105^+$ and $CD90^-CD105^+$ cells compared to the non-treated controls (Table, Fig. 2). At the same time, the content of p53-positive cells drastically increased ($p < 0.0001$ compared to non-treated cells).

The MCF-7 cells were also CD133-positive. The relative content of $CD133^+$ MCF-7 cells was higher as compared to MDA-MB-231 cells ($p < 0.01$), while MFI for CD133 in MCF-7 cells was lower (61.700 a.u. vs 120.938 a.u.). In contrast to MDA-MB-231 cells, the CD90, CD105, CD10, and p53 antigens were expressed by less than 1% of cells (Table 1). Moreover, a $CD90^+CD105^+$ population in the MCF-7 cells was lacking. The fraction of $Ki\text{-}67^+$ cells was low as compared to MDA-MB-231 cells. After SP treatment, we found some increase in the expression of CD10 antigen and p53, while Ki-67 expression did not change similarly to that in MDA-MB-231 cells.

To detect the possible modifying effect of SP on the irradiated cells, the cell samples of both cell lines were irradiated at 15 Gy following 48-h incubation with or without SP. Cell death, apoptosis, and cell cycle traverse were analyzed 24 h after radiation exposure. While the death of the MDA-MB-231 cells assessed by 7-AAD staining at the end of incubation with SP was negligible, the cell survival assessed by 7-AAD staining 24 h after irradiation slightly decreased. We did not observe the effect of SP on the decrease in the percent of the live cells 24 h after irradiation (Fig. 3).

The apoptotic cell death was assessed by the percent of cells in the sub-G1 phase following 3 days from the beginning of the experiment. The treatment of MDA-MB-231 cells with SP only did not show an increase in the apoptotic cell number (Fig. 4). In the samples exposed to radiation, the percent of apoptosis increased significantly both in MDA-MB-231 and MCF-7 cells. Nevertheless, 48-h SP pretreatment of MDA-MB-231 cells did not affect the apoptotic level induced by radiation

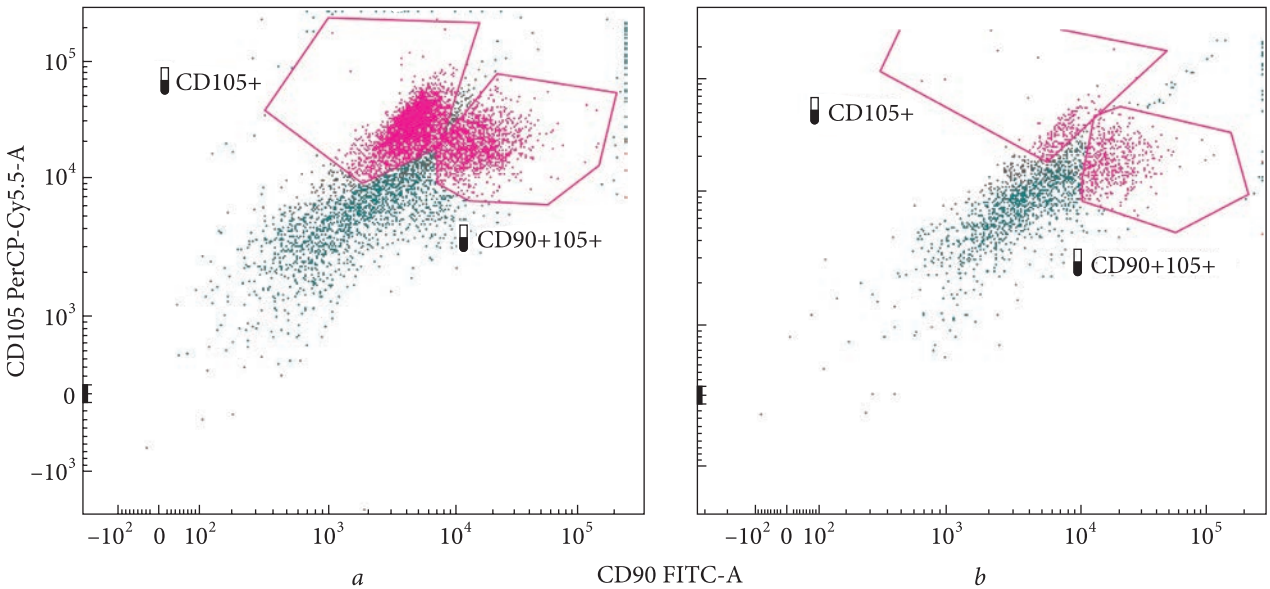

Fig. 2. Representative double color flow cytometry dot plots showing the expression of CD105 (PerCP-Cy5.5) and CD90 (FITC) antigens on MDA-MB-231 cells untreated (*a*) and treated by spike protein of SARS-Cov-2 (*b*)

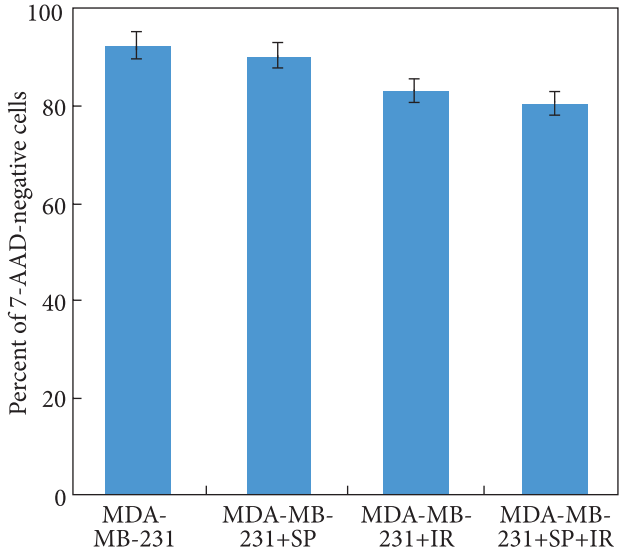

Fig. 3. Percentage of live MDA-MB-231 cells before and after irradiation. Cells were untreated or pretreated with SP of SARS-Cov-2 for 2 days before radiation exposure at 15 Gy. Cell suspensions were stained with 7-AAD viability staining solution and analyzed by flow cytometry

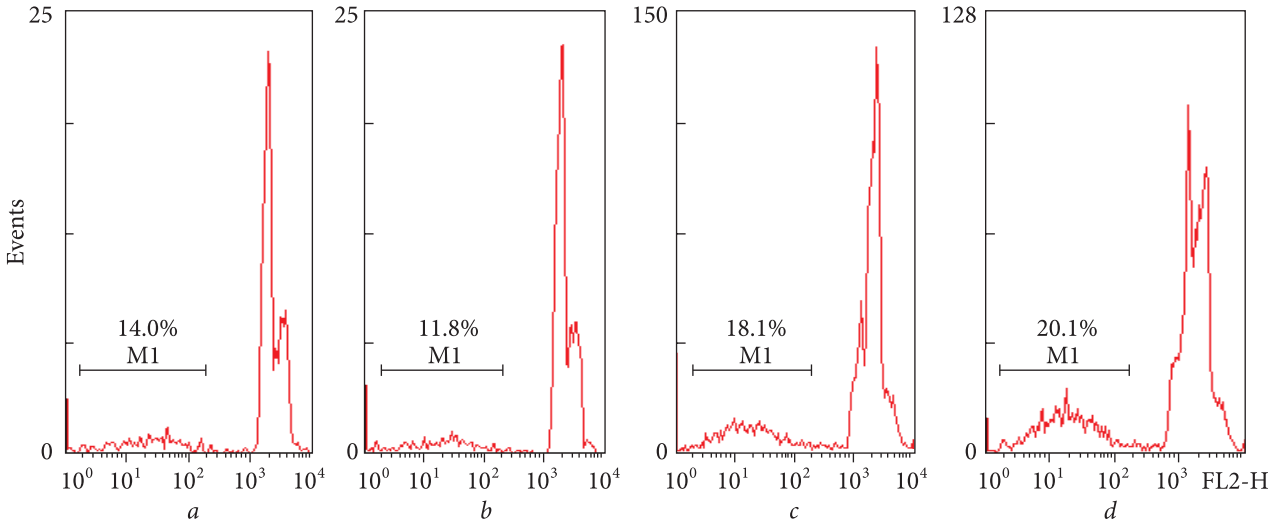

Fig. 4. Representative flow cytometry histograms of permeabilized MDA-MB-231 cells stained with propidium iodide: (*a*) control cells, (*b*) cells cultured with SP for 3 days, (*c*) cells cultured for 2 days without SP followed by irradiation at 15 Gy and further culture for 1 day, (*d*) cells cultured for 2 days with SP followed by irradiation at 15 Gy and further culture for 1 day. The M1 region of the histogram indicates sub-G1 cells. The percentage of cells in sub-G1 is shown. The total number of events analyzed for each condition was 10,000

(Fig. 4). At the same time, the radiation-induced apoptosis in MCF-7 cells pretreated with SP slightly increased (Fig. 5).

The expression of p53 significantly increased after irradiation of MDA-MB-231 cells regardless of whether they were pretreated with SP or not (90.3 ± ± 2.1% without SP treatment and 94.7 ± 3.1% in SP-treated cells). Nevertheless, the MFI was twice as high after SP treatment (18.407 a.u. and 34.784 a.u., correspondingly) (data not shown). It should be noticed that the baseline expression level of p53 in MCF-7 cells was almost an order of magnitude lower compared to MDA-MB-231 cells (see Table). Contrary to MDA-MB-231 cells, after irradiation, p53 expression remained low both in SP-treated and SP-untreated MCF-7 cells not exceeding 5—7% (data not shown).

The possible effects of SP and irradiation on cell cycle traverse were studied by analyzing the percentage of cells in the G0/G1, S, and G2/M phases of the cell cycle on the flow cytometry diagrams of PI-stained permeabilized cells. The results are shown as bar diagrams representing the corresponding percentage of cells in each phase of the cell cycle. As shown in Fig. 6, SP alone did not affect the cell cycle traverse in MDA-MB-231 cells. The radiation exposure resulted in the delay of the cell cycle with the accumulation of cells in the G2/M phase (from 18%

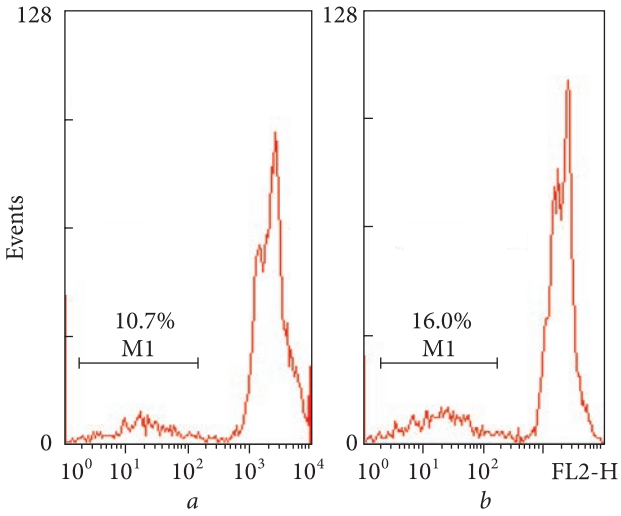

Fig. 5. Representative flow cytometry histograms of permeabilized MCF-7 cells stained with propidium iodide: (*a*) cells cultured for 3 days without SP followed by irradiation at 15 Gy and further culture for 1 day; (*b*) cells cultured for 2 days with SP followed by irradiation at 15 Gy and further culture for 1 day. The M1 region of the histogram indicates sub-G1 cells. The percentage of cells in sub-G1 is shown. The total number of events analyzed for each condition was 10,000

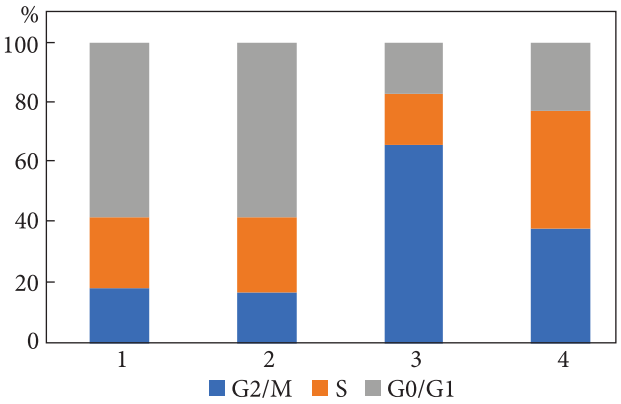

Fig. 6. Diagrams of cell cycle phase distribution plotted based on the results of the flow cytometric analysis of the distribution of permeabilized PI-stained MDA-MB-231 cells: 1 — control; 2 — cells cultured for 3 days without SP; 3 — cells cultured for 2 days without SP followed by irradiation at 15 Gy and further cultured for 1 day; 4 — cells cultured for 2 days with SP followed by irradiation at 15 Gy and further cultured for 1 day

in control to 66% in irradiated cells). Meanwhile, in SP-pretreated MDA-MB-231 cells, a drastic shift in the cell cycle phase distribution was evident. In particular, the S phase increased from by 17% in irradiated cells cultured without SP to by 39% in irradiated cells pretreated with SP.

An analogous pattern was evident for the cell cycle of MCF-7 cells. Similar to MDA-MB-231 cells, SP protein alone did not affect the distribution by cell cycle phases (data not shown). In irradiated MCF-7 cells, the noticeable cell accumulation in the G2/M phase was obvious. In SP-pretreated cells, the S phase increased from 27% in irradiated cells cultured without SP to 45% in irradiated cells pretreated with SP suggesting the slowdown of cell cycle progression (Fig. 7).

Discussion

In this study, we investigated the effect of SARS-Cov-2 SP on proliferative activity, immunophenotype and sensitivity to radiation-induced apoptosis in two BC cell lines, namely MDA-MB-231 and MCF-7, representing the TNBC and luminal A subtypes, respectively [23—25]. Both cell lines expressed angiotensin converting enzyme-2 receptor (weakly) and neuropilin 1 (strongly), which bind the SP and facilitate SARS-Cov-2 entry into the cells [26].

Unlike Johnson et al. [18] and Willson et al. [19], who noted the inhibition of the cancer cell line growth under the action of SARS-Cov-2 SP, we did not find any significant effect of SARS-Cov-2 SP on the proliferative activity of both studied cell lines in short-term incubation. No toxicity or apoptosis induction were found. At the same time, SP treatment altered the cell phenotype, especially in MDA-MB-231 cells.

The recent studies demonstrate that SARS-CoV-2 SP may elicit a global proteomic effect in cell culture even independently of interactions with the ACE2 receptor [27] Therefore, the study of the SP-induced changes in the expression of the antigens related to various intracellular pathways is important for elucidating various aspects of the pathogenesis of SARS-CoV-2 expression.

CD133, also known as prominin-1, a 120 kDa pentaspan glycoprotein with 5 transmembrane domains is considered a universal marker of organ-specific stem cells and tumor-initiating cells [28]. However, recent data suggests that CD133 expression is not restricted to organ-specific epithelial stem cells; on the contrary, CD133 is expressed in the differentiated epithelium. In particular, Liu et al. [29] did not find CD133 expression in the cells of normal breast tissue, but its expression increased with the progression of lesions from usual hyperplasia, through atypical ductal hyperplasia, ductal carcinoma in situ, and invasive carcinoma. Coincidentally,

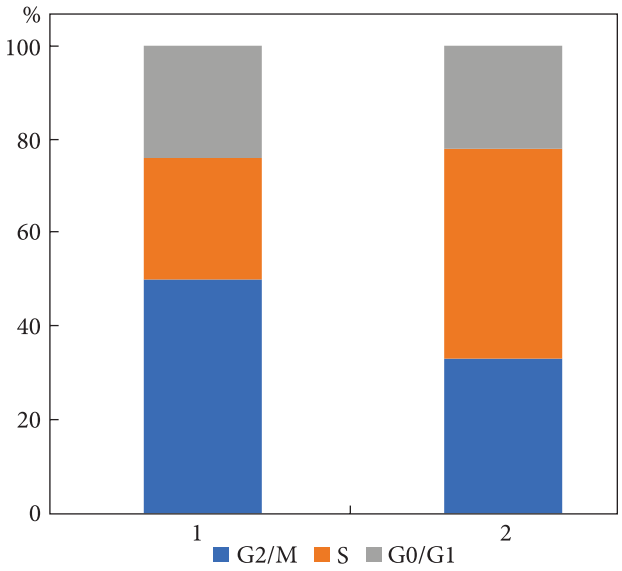

Fig. 7. Diagrams of cell cycle phase distribution plotted based on the results of the flow cytometric analysis of the distribution of permeabilized PI-stained MCF-7 cells: 1 — cells cultured for 2 days without SP followed by irradiation at 15 Gy and further cultured for 1 day; 2 — cells cultured for 2 days with SP followed by irradiation at 15 Gy and further cultured for 1 day

CD133 colocalized with cell membrane–bound SARS-CoV-2 SP and may contribute to SARS-CoV-2 infection in ACE2-expressing cells [30]. In our study, the percent of CD133-positivity was higher in MCF-7 cells compared to MDA-MB-231 cells, while fluorescence intensity in MCF-7 cells was significantly lower. Nevertheless, no changes in CD133 expression under SP treatment were detected.

CD90 (Thy-1 antigen) is a mesenchymal stem cell marker, associated with malignancy degree of the cell lines [31]. Higher expression of CD105 (endoglin) on mammary cancer cells is associated with poor overall and disease-free survival of patients [32]. In our study, about 30% of SP-untreated MDA-MB-231 cells co-expressed CD90 and CD105 antigens. Wang et al. [33] showed that a $CD105^+$ $CD90^+$ fraction of MDA-MB-231 cells is a highly proliferative and migratory subpopulation with "mesenchymal stem cell-like" characteristics. The expression of CD105 and CD90 was significantly reduced after SP treatment, which may affect the phenotypic properties of the cells resulting in their lower migratory and invasive abilities.

The p53 protein expression increased both in MDA-MB-231 and MCF-7 cells treated with SP. This is consistent with the data of Lee et al. [34] who showed that SARS-Cov-2 infection leads to the stabilization of p53 protein in Vero E6 cells. Zhang et al. [35] found that in the presence of SP, p53 degradation in different cancer cell lines (including MCF-7) was reduced due to disruption of p53-MDM2 interaction, which is necessary for ubiquitination and subsequent proteasomal degradation of p53. Nevertheless, at the same time, SP inhibited chemotherapy-induced p53 gene activation of p21 (WAF1), TRAIL Death Receptor DR5 and MDM2. Willson et al. [18] obtained opposite data and showed that the anti-proliferative effect of SARS-Cov-2 SP on SiHa cervical cancer cells was associated with the up-regulation of p53, and the pro-apoptotic effect of SP was associated with the up-regulation of TRAIL. Such different data highlight the need for further study of the effects of SP and other SARS-Cov-2 proteins on p53- and p53-related signaling pathways.

In our opinion, the differences in the percent of p53-positive cells in the studied BC cell lines may be related to the expression of mutant gain-of-function p53-R280K in MDA-MB-231 cells [36]. This mutation affects the DNA binding domain, abrogates the normal instability of the protein, and leads to massive accumulation of the steady-state mutant p53 protein [37, 38]. MCF-7 cells have two normal copies of the p53 gene with half-life as short as a few minutes [39, 40].

Radiotherapy is widely used in the treatment of BC patients. BC cell lines can be used as a model for studying the mechanisms of radiation-induced apoptosis to find ways to an increase in the radiosensitivity of malignant cells. In some studies, the MCF-7 cell line was more radioresistant than the MDA-MB-231 cell line at 4 h and 24 h after X-ray irradiation [41], while in some others, the radiosensitivity of cell lines did not differ significantly [42], or the apoptosis rate of MCF-7 cells was significantly higher than that of MDA-MB-231 cells at doses of 2, 4, and 8 Gy [43]. In the setting of our experiments, irradiation at a dose of 15 Gy results in a slight increase in the percent of hypodiploid cells in both cell lines under study. SP had some pro-apoptotic effect on both cell lines, but it was not pronounced. In irradiated MDA-MB-231, but not MCF-7 cells, the p53 expression increased compared to the baseline values. Meanwhile, the percent of p53-positive MDA-MB-231 cells upon irradiation was essentially the same regardless of whether they were pretreated with SP or not, although the expression level was significantly high-

er in SP-treated cells. This is in line with the above-mentioned data on the ability of SP to stabilize p53.

An important effect of SP treatment demonstrated in our study was a significant increase in cells in the S-phase in irradiated MDA-MB-231 and MCF-7 cells. Huang et al. [44] showed that ionizing radiation increases the expression of the E2F-1 transcription factor and the entry of cells into the S phase followed by apoptosis. The overexpression of E2F-1 or inhibition of cyclin A/cdk2 phosphorylation of E2F-1 in fibroblasts has been associated with the S-phase delay and subsequent apoptosis without any additional pro-apoptotic stimuli [45, 46]. Enhanced E2F-1 transcriptional activity associated with the S-phase arrest and subsequent apoptosis was observed in mammary epithelial cell lines treated by a synthetic retinoid-like compound [47]. On the other hand, treatment of alveolar type II (ATII)-like rat L2 cells with SP upregulated the activity of the phosphorylated forms of E2F-1, which leads to a significant increase in the S phase accumulation with a concomitant decrease in the G2 phase as compared with the nontreated control [27]. Summarizing these data, we may suppose that SP-treatment of MDA-MB-231 and MCF-7 cells leads to an increase in E2F-1 activity, which is realized in the S-phase delay during subsequent irradiation. Interestingly, we did not observe any changes in the proliferative activity or cell cycle traverse in SP-treated cells without irradiation.

In conclusion, we did not detect any effect of SARS-Cov-2 SP on the proliferation of MDA-MB-231 and MCF-7 cells. Nevertheless, some changes in the phenotype of MDA-MB-231 cells treated with SARS-Cov-2 SP were evident, in particular, a decrease in the content of $CD105^+CD90^+$ and $CD105^+CD90^-$ subpopulations. Furthermore, SP is involved in the S-phase delay after irradiation of the cells. The reasons for such a delay in cell cycle traverse such as a presumable involvement of E2F-1 deserve further studies. The obtained data might have a certain significance in the study of the effect of anti-SARS-Cov-2 vaccination on tumor growth since most vaccines are based on SP expression. However, *in vivo* effects may also depend on other factors (in particular, the activating effect of SP on immune system cells). Therefore, further studies of such effects are worthwhile.

Acknowledgment

The authors are grateful to Mr. Thomas Harms, President of Charitable Organization "KIHEW-KInderhilfe" (Germany) who provided support by reagents for the fulfillment of the work.

REFERENCES

1. Lechner-Scott J, Levy M, Hawkes C, et al. Long COVID or post COVID-19 syndrome. *Mult Scler Relat Disord*. 2021;55:e103268. https://doi.org/10.1016/j.msard.2021.103268
2. Ståhlberg M, Reistam U, Fedorowski A, et al. Post-COVID-19 tachycardia syndrome: a distinct phenotype of post-acute COVID-19 syndrome. *Am J Med*. 2021;134(12):1451-1456. https://doi.org/10.1016/j.amjmed.2021.07.004
3. Roy S, Demmer RT. Impaired glucose regulation, SARS-CoV-2 infections and adverse COVID-19 outcomes. *Transl Res*. 2022;241:52-69. https://doi.org/10.1016/j.trsl.2021.11.002
4. Gyöngyösi M, Alcaide P, Asselbergs FW, et al. Long COVID and the cardiovascular system-elucidating causes and cellular mechanisms in order to develop targeted diagnostic and therapeutic strategies: a joint Scientific Statement of the ESC Working Groups on Cellular Biology of the Heart and Myocardial and Pericardial Diseases. *Cardiovasc Res*. 2023;119(2):336-356. https://doi.org/10.1093/cvr/cvac115
5. Gracia-Ramos AE, Saavedra MA. Systemic lupus erythematosus after SARS-CoV-2 infection: a causal or temporal relationship? *Int J Rheum Dis*. 2023;26(12):2373-2376. https://doi.org/10.1111/1756-185X.14896
6. Martini N, Singla P, Arbuckle E, et al. SARS-CoV-2-induced autoimmune hepatitis. *Cureus* 2023;15(5):e38932. https://doi.org/10.7759/cureus.38932
7. Liu Y, Sawalha AH, Lu Q. COVID-19 and autoimmune diseases. *Curr Opin Rheumatol*. 2021;33(2):155-162. https://doi.org/10.1097/BOR.0000000000000776
8. Aboueshia M, Hussein MH, Attia AS, et al. Cancer and COVID-19: analysis of patient outcomes. *Future Oncol*. 2021;17(26):3499-3510. https://doi.org/10.2217/fon-2021-0121
9. Mato AR, Roeker LE, Lamanna N, et al. Outcomes of COVID-19 in patients with CLL: a multicenter international experience. *Blood*. 2020;136(10):1134-1143. https://doi.org/10.1182/blood.2020006965
10. Salvatore M, Hu MM, Beesley LJ, et al. COVID-19 outcomes by cancer status, site, treatment, and vaccination. *Cancer Epidemiol Biomarkers Prev*. 2023;32(6):748-759. https://doi.org/10.1158/1055-9965.EPI-22-0607
11. Sawyers A, Chou M, Johannet P, et al. Clinical outcomes in cancer patients with COVID-19. *Cancer Rep (Hoboken)*. 2021;4(6):e1413. https://doi.org/10.1002/cnr2.1413

12. Jahankhani K, Ahangari F, Adcock IM, Mortaz E. Possible cancer-causing capacity of COVID-19: Is SARS-CoV-2 an oncogenic agent? *Biochimie.* 2023;213:130-138. https://doi.org/10.1016/j.biochi.2023.05.014
13. Li J, Bai H, Qiao H, et al. Causal effects of COVID-19 on cancer risk: a Mendelian randomization study. *J Med Virol.* 2023;95(4):e28722. https://doi.org/10.1002/jmv.28722
14. Popov V, Bumbea H, Andreescu M, et al. Is COVID-19 infection a trigger for progression of CLL? *Clin Lymphoma Myeloma Leuk.* 2022;22:S260. https://doi.org/10.1016/S2152-2650(22)01313-1
15. Gluzman DF, Zavelevich MP, Philchenkov AA, et al. Immunodeficiency-associated lymphoproliferative disorders and lymphoid neoplasms in post-COVID-19 pandemic era. *Exp Oncol.* 2021;43(1):87-91. https://doi.org/10.32471/exp-oncology.2312-8852.vol-43-no-1.15795
16. Dyagil IS, Abramenko IV, Martina ZV, et al. The course of chronic lymphocytic leukemia after SARS-CoV-2 virus infection. *Probl Radiac Med Radiobiol.* 2023;28:267-276. https://doi.org/10.33145/2304-8336-2023-28-267-276
17. Nguyen HT, Kawahara M, Vuong CK, et al. SARS-CoV-2 M protein facilitates malignant transformation of breast cancer cells. *Front Oncol.* 2022;12:e923467. https://doi.org/10.3389/fonc.2022.923467
18. Johnson BD, Zhu Z, Lequio M, et al. SARS-CoV-2 spike protein inhibits growth of prostate cancer: a potential role of the COVID-19 vaccine killing two birds with one stone. *Med Oncol.* 2022;39(3):e32. https://doi.org/10.1007/s12032-021-01628-1
19. Willson CM, Lequio M, Zhu Z, et al. The role of SARS-CoV-2 spike protein in the growth of cervical cancer cells. *Anticancer Res.* 2024;44(5):1807-1815. https://doi.org/10.21873/anticanres.16982
20. Vitiello A, Ferrara F, Auti AM, et al. Advances in the Omicron variant development. *J Intern Med.* 2022;292(1):81-90. https://doi.org/10.1111/joim.13478
21. Feoktistova M, Geserick P, Leverkus M. Crystal violet assay for determining viability of cultured cells. *Cold Spring Harb Protoc.* 2016;2016(4):pdb.prot087379. https://doi.org/10.1101/pdb.prot087379
22. Riccardi C, Nicoletti I. Analysis of apoptosis by propidium iodide staining and flow cytometry. *Nat Protoc.* 2006;1(3):1458-1461. https://doi.org/10.1038/nprot.2006.238
23. Kumar P, Aggarwal R. An overview of triple-negative breast cancer. *Arch Obstet Gynaecol.* 2016;293(2):247-269. https://doi.org/10.1007/s00404-015-3859-y
24. Dias K, Dvorkin-Gheva A, Hallett RM, et al. Claudin-low breast cancer; clinical & pathological characteristics. *PLoS One.*2017;12(1):e0168669. https://doi.org/10.1371/journal.pone.0168669
25. Holliday DL, Speirs V. Choosing the right cell line for breast cancer research. *Breast Cancer Res.* 2011;13(4):e215. https://doi.org/10.1186/bcr2889
26. Sommariva M, Dolci M, Triulzi T, et al. Impact of in vitro SARS-CoV-2 infection on breast cancer cells. *Sci Rep.* 2024;14(1):e13134. https://doi.org/10.1038/s41598-024-63804-3
27. Mobley JA, Molyvdas A, Kojima K, et al. The SARS-CoV-2 spike S1 protein induces global proteomic changes in ATII-like rat L2 cells that are attenuated by hyaluronan. *Am J Physiol Lung Cell Mol Physiol.* 2023;324(4):L413-L432. https://doi.org/10.1152/ajplung.00282.2022
28. Li Z. CD133: a stem cell biomarker and beyond. *Exp Hematol Oncol.* 2013;2(1):17. https://doi.org/10.1186/2162-3619-2-17
29. Liu TT, Li XF, Wang L, Yang JL CD133 expression and clinicopathologic significance in benign and malignant breast lesions. *Cancer Biomark.* 2020;28(3):293-239. https://doi.org/10.3233/CBM-190196
30. Kotani N, Nakano T, Kuwahara R. Host cell membrane proteins located near SARS-CoV-2 spike protein attachment sites are identified using proximity labeling and proteomic analysis. *J Biol Chem*. 2022;298(11):102500. https://doi.org/10.1016/j.jbc.2022.102500
31. Lobba ARM, Carreira ACO, Cerqueira OLD, et al. High CD90 (THY-1) expression positively correlates with cell transformation and worse prognosis in basal-like breast cancer tumors. *PLoS One.* 2018;13(6):e0199254. https://doi.org/10.1371/journal.pone.0199254
32. Davidson B, Stavnes HT, Førsund M, et al. CD105 (Endoglin) expression in breast carcinoma effusions is a marker of poor survival. *Breast.* 2010;19(6):493-498. https://doi.org/10.1016/j.breast.2010.05.013
33. Wang X, Liu Y, Zhou K, et al. Isolation and characterization of CD105+/CD90+ subpopulation in breast cancer MDA-MB-231 cell line. *Int J Clin Exp Pathol.* 2015;8(5):5105-5112.
34. Lee JD, Menasche BL, Mavrikaki M, et al. Differences in syncytia formation by SARS-CoV-2 variants modify host chromatin accessibility and cellular senescence via TP53. *Cell Rep.* 2023;42(12):e113478. https://doi.org/10.1016/j.celrep.2023.113478
35. Zhang S, El-Deiry WS. Transfected SARS-CoV-2 spike DNA for mammalian cell expression inhibits p53 activation of p21(WAF1), TRAIL Death Receptor DR5 and MDM2 proteins in cancer cells and increases cancer cell viability after chemotherapy exposure. *Oncotarget.* 2024;15:275-284. https://doi.org/10.18632/oncotarget.28582
36. Bae YH, Shin JM, Park HJ, et al. Gain-of-function mutant p53-R280K mediates survival of breast cancer cells. *Genes Genom.* 2014;36:171-178. https://doi.org/10.1007/s13258-013-0154-9
37. Gomes AS, Trovão F, Andrade Pinheiro B, et al. The crystal structure of the R280K mutant of human p53 explains the loss of DNA binding. *Int J Mol Sci.* 2018;19(4):e1184. https://doi.org/10.3390/ijms19041184
38. Frum RA, Grossman SR. Mechanisms of mutant p53 stabilization in cancer. *Subcell Biochem.* 2014;85:187-197. https://doi.org/10.1007/978-94-017-9211-0_10

39. Balcer-Kubiczek EK, Yin J, Lin K, et al. p53 mutational status and survival of human breast cancer MCF-7 cell variants after exposure to X rays or fission neutrons. *Radiat Res.* 1995;142(3):256-262
40. Maltzman W, Czyzyk L. UV irradiation stimulates levels of p53 cellular tumor antigen in nontransformed mouse cells. *Mol Cell Biol.* 1984;4(9):1689-1694. https://doi.org/10.1128/mcb.4.9.1689-1694.1984
41. Mahmoud A, Casciati A, Bakar ZA, et al. The detection of DNA damage response in MCF7 and MDA-MB-231 breast cancer cell lines after X-ray exposure. *Genome Integr.* 2023;14:e1. https://doi.org/10.14293/genint.14.1.001
42. Hargrave SD, Joubert AM, Potter BVL, et al. Cell fate following irradiation of MDA-MB-231 and MCF-7 breast cancer cells pre-exposed to the tetrahydroisoquinoline sulfamate microtubule disruptor STX3451. *Molecules.* 2022;27(12):e3819. https://doi.org/10.3390/molecules27123819
43. Sun L, Zhang S, Chen G. Effect of radiation-induction on cell cycle and apoptosis in breast cancer cell lines MDA-MB-231 and MCF-7. *Cancer Res Clinic.* 2018;**6**:511-515
44. Huang Y, Ishiko T, Nakada S, et al. Role for E2F in DNA damage-induced entry of cells into S phase. *Cancer Res.* 1997;57(17):3640-3643. PMID: 9288762.
45. Qin XQ, Livingston DM, Kaelin WG Jr, Adams PD. Deregulated transcription factor E2F-1 expression leads to S-phase entry and p53-mediated apoptosis. *Proc Natl Acad Sci U S A.* 1994;91(23):10918-10922. https://doi.org/10.1073/pnas.91.23.10918
46. Shan B, Lee WH. Deregulated expression of E2F-1 induces S-phase entry and leads to apoptosis. *Mol Cell Biol.* 1994;14(12):8166-8173. https://doi.org/10.1128/mcb.14.12.8166-8173.1994
47. Zhang Y, Rishi AK, Dawson MI, et al. S-phase arrest and apoptosis induced in normal mammary epithelial cells by a novel retinoid. *Cancer Res.* 2000;60(7):2025-2032. PMID: 10766194

Submitted: January 8, 2025

В. Бриченко [1], Л. Шлапацька [2], М. Завелевич [2], Л. Зварич [1], В. Панченко [1],
О. Лясківська [1], О. Скачкова [3], Н. Голярник [1], І. Абраменко [1], Л. Бучинська [2], А. Чумак [1]

[1] Національний науковий центр радіаційної медицини, гематології та онкології Національної Академії медичних наук України, Київ, Україна
[2] Інститут експериментальної патології, онкології і радіобіології ім. Р.Є. Кавецького Національної Академії наук України, Київ, Україна
[3] Державне некомерційне підприємство «Національний Інститут раку», Київ, Україна

ВПЛИВ СПАЙК БІЛКА ВІРУСУ SARS-COV-2 НА РІСТ ТА ФЕНОТИП КЛІТИН MDA-MB-231 І MCF-7 РАКУ МОЛОЧНОЇ ЗАЛОЗИ ТА ЇХНЮ ЧУТЛИВІСТЬ ДО АПОПТОЗУ, ІНДУКОВАНОГО ІОНІЗУЮЧИМ ВИПРОМІНЕННЯМ

Стан питання. Коронавірусна інфекція, спричинена штамом вірусу SARS-Cov-2, крім важкого гострого респіраторного синдрому, призводить до розвитку синдрому мультиорганної патології. Значна увага приділяється її взаємозв'язку з онкологічними захворюваннями. Дані клінічних та експериментальних досліджень на теперішній час є суперечливими. Необхідні подальші дослідження для уточнення потенційного впливу SARS-Cov-2 на пухлинні клітини. **Мета**: дослідити вплив спайк-білка (СБ) SARS-Cov-2 на виживаність, фенотип та чутливість до апоптозу, індукованого дією іонізуючого випромінення (ІВ), клітин ліній MDA-MB-231 і MCF-7 раку молочної залози. **Матеріали та методи**. Дослідження впливу СБ SARS-Cov-2 на ріст клітин ліній MDA-MB-231 і MCF-7 раку молочної залози проводили за допомогою проліферативного тесту з використанням кристалічного фіолетового. Профіль експресії Ki-67, CD44, CD133, CD105, CD90, CD10, CD5, CD19 та p53 досліджували методом протокової цитометрії. Чутливість до ІВ-індукованого апоптозу оцінювали за забарвленням трипановим синім, 7-аміно-актиноміцином D та пропідій йодидом. **Результати**. Не виявлено суттєвого впливу СБ на проліферативну активність обох клітинних ліній при короткостроковому культивуванні. Після обробки СБ в клітинах лінії MDA-MB-231 зменшувався вміст субпопуляцій $CD105^+CD90^+$ та $CD105^+CD90^-$ клітин ($p < 0,0001$). Експресія p53 підвищувалась в обох лініях. Виявлена тенденція до підвищення чутливості клітин MDA-MB-231 і MCF-7 до ІВ-індукованого апоптозу. В обох опромінених культурах виявлено збільшення клітин в S-фазі після обробки СБ порівняно з необробленими клітинами. Індукція апоптозу в клітинах лінії MDA-MB-231 супроводжувалась значним підвищенням експресії p53; зміни були більш виразними після обробки СБ. Експресія p53 після опромінення залишалась низькою в клітинах лінії MCF-7 незалежно від впливу СБ. **Висновок**. Не виявлено посилення росту клітин пухлинних ліній MDA-MB-231 і MCF-7 під впливом СБ SARS-Cov-2. Отримані дані можуть мати певне значення для дослідження впливу на пухлинні клітини вакцинації проти SARS-Cov-2 вірусу, оскільки більшість сучасних вакцин базується на експресії СБ. Однак, ефекти in vivo можуть залежати і від інших факторів (насамперед, активуючого впливу СБ на клітини імунної системи).

Ключові слова: MDA-MB-231, MCF-7 клітинні лінії, SARS-Cov-2. спайк білок. імунофенотип, апоптоз, індукований дією іонізуючого випромінення.